

LA-7618-MS

Informal Report

MASTER

Stability Theory for Internal Ring Configurations

University of California



LOS ALAMOS SCIENTIFIC LABORATORY

Post Office Box 1663 Los Alamos, New Mexico 87545

Stability Theory for Internal Ring Configurations

Guthrie Miller

NOTICE

This report was prepared as an account of work sponsored by the United States Government. Neither the United States nor the United States Department of Energy, nor any of their employees, nor any of their contractors, subcontractors, or their employees, makes any warranty, express or implied, or assumes any legal liability or responsibility for the accuracy, completeness or usefulness of any information, apparatus, product or process disclosed, or represents that its use would not infringe privately owned rights.



STABILITY THEORY FOR INTERNAL RING CONFIGURATIONS

by

Guthrie Miller

ABSTRACT

The magnetohydrodynamic stability theory of internal ring configurations is developed using a nearly cylindrical, sharp-boundary plasma model.

I. INTRODUCTION

In this report the stability of a straight configuration with internal rings is investigated. As these configurations are positively stable (in contrast to the neutrally stable theta pinch), the configuration can be imagined to be bent into a torus or a U bend. The positive stability is not altered if the radius of curvature is large enough.

The internal ring experimental work at Nagoya^{1,2} was based on $\int d\ell/B$ theory, which is a low- β concept. The closely related problem of stability of the main plasma in ELMO has been solved for arbitrary β ,³ and illustrates how the $\int d\ell/B$ criterion generalizes to high β . The ELMO theory is necessarily rather complicated because of the many degrees of freedom inherent in a diffuse profile. Here, a sharp-boundary, small- δ model is used to obtain, in a relatively simple manner, an overall impression of the stability properties of internal ring configurations. The model is first discussed in a general way, for arbitrary axisymmetric fixed internal currents, and then applied to internal rings. It is also of interest to check the model for the case of ELMO

to see that the predictions are in basic agreement with the more complete theory.

II. SHARP-BOUNDARY THEORY

A sharp-boundary, small- δ theory, analogous to that used for the high-beta stellarator, can be used to describe fixed internal current configurations.⁴ Simplicity is the main justification for the assumptions that are made. These assumptions are (1) a sharp boundary, which means that the equilibrium has only a single parameter β , and (2) near-cylindrical geometry, which allows the modes to be characterized in terms of cylindrical k and m values.

The basic equilibrium consists of a cylindrical plasma of radius a with external field B_0 and internal field $(1-\beta)^{1/2}B_0$. This situation is perturbed by fixed axisymmetric internal and external currents on the surfaces $r = b$ and $r = d$, with $b < a < d$. As a result of the perturbation, the plasma surface deforms and assumes the shape

$$r = a \left[1 + \sum_h \delta_h \cos(hz) \right] \quad . \quad (1)$$

The deformation parameters δ are given in terms of the Fourier components of the fixed currents j_d and j_b as follows

$$\delta = \delta_e + \delta_i \quad ,$$

$$\delta_e = - \frac{d j_d I_0'(ha) K_0'(hd)}{B_0 a [1 + \beta h a I_0(ha) K_0'(ha)]} \quad ,$$

$$\delta_i = - \frac{(1-\beta)^{1/2} b j_b I_0'(hb) K_0'(ha)}{B_0 a [1 + \beta h a I_0(ha) K_0'(ha)]} \quad . \quad (2)$$

The growth rate (or oscillation frequency) of an arbitrary m , $k = 0$ mode is given by

$$\gamma^2 = \frac{T_e + T_i}{M} \sum_{\mathbf{k}} h^2 \delta^2 \left\{ 2x^2 f - 1 + \frac{\beta}{1-\beta} \frac{(1-\beta)(1 + 2x^2 f I^m) + x^4 f^2 I^m K^m}{I^m(1-\beta) - K^m} \right\} \quad , \quad (3)$$

where M is the ion mass, and f is defined by

$$f = (1-\beta)I^0 \frac{\delta_e}{\delta} + K^0 \frac{\delta_i}{\delta} \quad , \quad (4)$$

with $x \equiv ha$, $I^0 \equiv I_0(x)/(xI_0'(x))$, and $K^0 \equiv K_0(x)/(xK_0'(x))$.

Equation (3) has interesting limits that should be noted. For $\beta \rightarrow 0$, only the first term in the brackets survives. This term is independent of m and is, in fact, just the derivative with respect to flux of $\int d\ell/B$ or V'' , since

$$\frac{2\pi B_0^2 V''}{L} = \sum_{\mathbf{k}} h^2 \delta^2 (2x^2 f - 1) \quad . \quad (5)$$

For $m \rightarrow \infty$, $I^m \rightarrow 1/m$ and $K^m \rightarrow -1/m$. In this limit, for $\beta < 1$, the second term in brackets approaches $m\beta/(2-\beta)$. Since this is an arbitrarily large destabilizing term, high- m modes are always unstable. However, very high m -number modes would be stabilized by gyro-viscosity, because the stability criterion,⁵

$$\gamma < \frac{m(m-1)T_i}{2eB_0(1-\beta)^{1/2}a^2} \quad , \quad (6)$$

is always satisfied for large enough m .

III. INTERNAL RING CONFIGURATIONS

With internal currents carried by slender rings, the current density is given by

$$j_{\theta} = I \delta(r-b) \sum_{i=-\infty}^{\infty} \delta(z-iL) = \delta(r-b) \sum_n j_n \cos\left(\frac{2\pi n z}{L}\right) \quad , \quad (7)$$

and the Fourier amplitude for $h = 2\pi n/L$ is $j_n = 2I/L$, independently of n . The summation in Eq. (3) is exponentially convergent and can readily be carried out. The result for the oscillation frequency ω for an arbitrary m , $k = 0$ mode can be written as

$$\omega^2 = \frac{T_e + T_i}{M} \left(\frac{I}{B_0 a}\right)^2 \frac{\sigma}{a^2} \quad , \quad (8)$$

where σ is a function of m , β , L/a , and b/a .

In Fig. 1 the stability boundary in m - β space is plotted for several geometries. Instability occurs only for large values of m , and for typical (theta pinch) experimental parameters would be stabilized by gyro-viscosity (stabilization requires a sufficiently small line density).

The stability of the $k = 0$, $m = 1$ mode allows the configuration to be bent into a large-radius torus or U bend. Toroidal equilibrium is the result of a balance between the toroidal force F_R and the $m = 1$ restoring force proportional to $\omega^2 \xi$, where ξ is the toroidally outward shift. The ring current necessary for equilibrium in a torus of radius R is given by

$$I = B_0 a \left(\frac{2a^2}{\sigma \xi R}\right)^{1/2} \quad . \quad (9)$$

In practical units $B_0 a$ is a current in Amperes equal to $0.8 B_0 [G] a [cm]$. Fig. 2 shows a plot of $\sigma|_{m=1}$ vs various parameters. Figure 2 allows the ring current to be obtained for cases of interest using Eq. (9). The strong

stabilizing effect of having the plasma radius nearly equal to the ring radius, that is, b/a near 1, is evident in Fig. 2.

Figure 3 gives field line plots for $L = b$ and $I = B_0 L$ (Fig. 3a), and $I = 3B_0 L$ (Fig. 3b). Also shown are the values of $B_0 V' / L$ associated with each flux surface. Using Eq. (9), these configurations could be bent into tori or U bends with radii $R = 70a$ and $R = 8a$, respectively, for the cases shown in Figs. 3a and 3b, with $\xi = 0.15a$, $\beta = 0.5$, and $b/a = 0.85$.

The sharp-boundary, small- δ theory does not distinguish the sign of the ring current. Field line plots such as Fig. 3 show that when the ring-produced current is in the same direction as the main field (the Fig. 3 case), there is a separatrix outside the ring, whereas when the ring-produced field opposes the main field, there is a separatrix inside the ring. In both cases V'' is negative for flux surfaces outside the separatrix and positive inside. For small currents the critical flux surface is essentially at the ring radius.

IV. ELMO

As a check, and to illustrate the relationship that exists between internal ring devices and ELMO, the sharp-boundary theory can be applied to ELMO. In ELMO, the hot-electron annuli are treated as rigid objects and their diamagnetic currents serve as the fixed internal current. The geometry is shown in Fig. 4.

The hot-electron current in ELMO consists of two azimuthal current sheets flowing in opposite directions on the inside and outside of the annulus. Assuming that the spacing between the sheets w (see Fig. 4) is small, the effective Fourier components of the current, considered as a simple current at $r = b$, are given by

$$j_n^{\text{eff}} = \frac{2I}{L} (-1)^n \sin\left(\frac{n\pi\ell}{L}\right) \frac{2w}{\ell} \frac{I_0(2\pi nb/L)}{I_0'(2\pi nb/L)} \quad (10)$$

The Fourier amplitudes describing the external current at $r = d$ are independent of n and are given by

$$j_n = \frac{2I_0}{L} = 2B_0 \quad . \quad (11)$$

Using these currents, Eq. (3) is again a convergent sum, which can be evaluated to determine γ^2 . In Fig. 5 the stability boundaries for modes with different m values are shown for a fixed geometry (that illustrated in Fig. 4). In the sharp-boundary model, high- m -number modes are always unstable for $\beta > 0$. However, from Fig. 5 it is possible to have high β and a large number of stable modes, e.g., $m < 30$, if the hot-electron current is large enough. Also shown in Fig. 5 is the stability boundary for $m = 30$ and $l/a = 0.3$, that is, a shorter length hot-electron annulus.

The diffuse-profile theory of ELMO³ gives similar behavior except that there is absolute stability, as shown in Fig. 6 (taken from Ref. 3). High- m -number modes are the most dangerous; however, with a diffuse profile the modes do not continue to become more unstable with m as they do with a sharp boundary. The effect of a short vs long annulus is similar in the diffuse-profile and sharp-boundary theories.

The threshold value of β_1 for $\beta = 0$ in Figs. 5 and 6 is determined by the internal current necessary to give negative V'' at the plasma surface. It is important to note that in a system without external field perturbations (e.g., as discussed in Sec. III), there is no such threshold and stability is achieved for an arbitrarily small internal current.

REFERENCES

1. T. Uchida, K. Sato, N. Noda, T. Aizawa, Y. Osanai, T. Itagaki, and R. Akijama, "A keV Collisionless Theta-Pinch Plasma Confined in the Caulked-Cusp Torus (CCT) Field," *Plas. Phys. & Controlled Nucl. Fusion Res.*, 1974, Vol. III., p.161 (1975).
2. T. Uchida, K. Sato, A. Mohri, and R. Akizawa, "Confinement of a Toroidal Theta-Pinch Plasma in a Periodic Caulked-Cusp Field," *Plas. Phys. & Controlled Nucl. Fusion Res.*, 1971, Vol. III., p.169 (1971).

3. D.B. Nelson and C.L. Hedrick, "Macroscopic Stability and β Limits in the ELMO Bumpy Torus," Oak Ridge Scientific Laboratory report ORNL/TM-5967 (1977).
4. G. Miller, "Magnetohydrodynamics of Nearly Cylindrical Configurations With Fixed Internal Currents," Phys. Fluids (to be published).
5. G. Miller, "On Plasma Transport and Flow in the Fluid Picture," Los Alamos Scientific Laboratory report LA-7429-MS (1978).

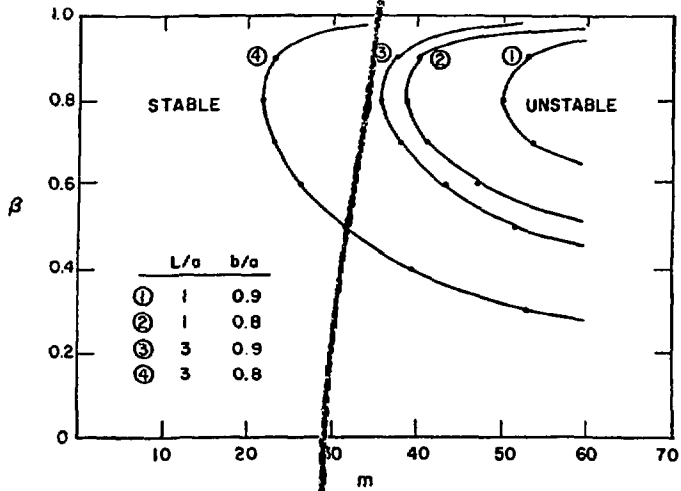


Fig. 1.
Stability of an internal ring configuration as a function of β and m , for several geometries.

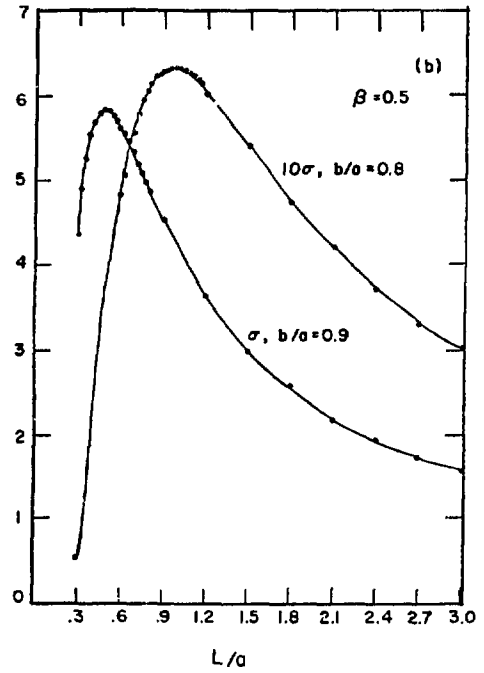
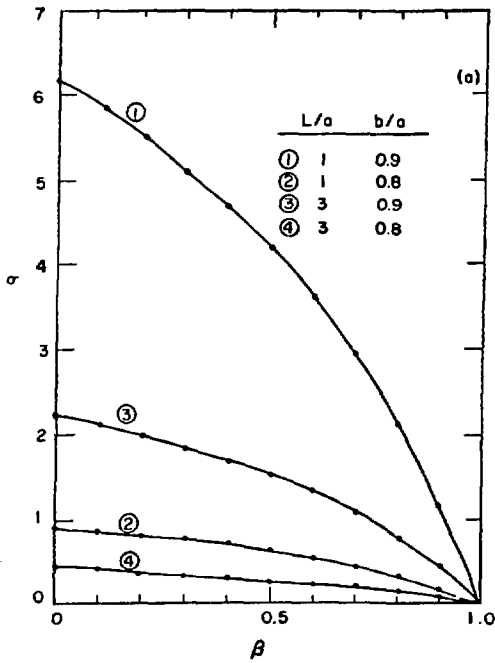


Fig. 2.
The normalized oscillation frequency of the $m = 1$ mode. In (a) σ is plotted vs β for configurations with different geometries, and in (b) it is plotted vs L/a for $\beta = 0.5$ and different b/a values.

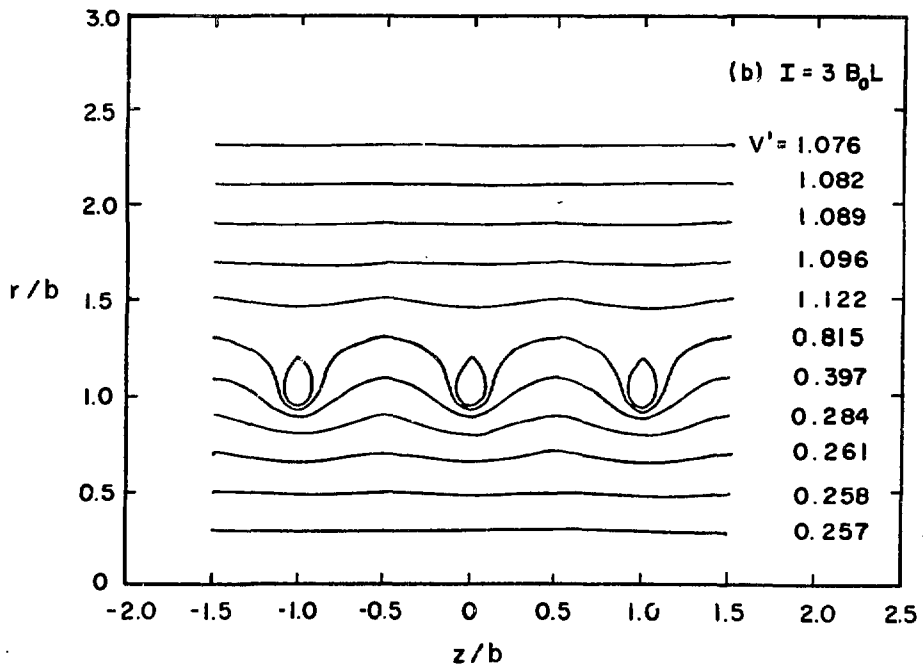
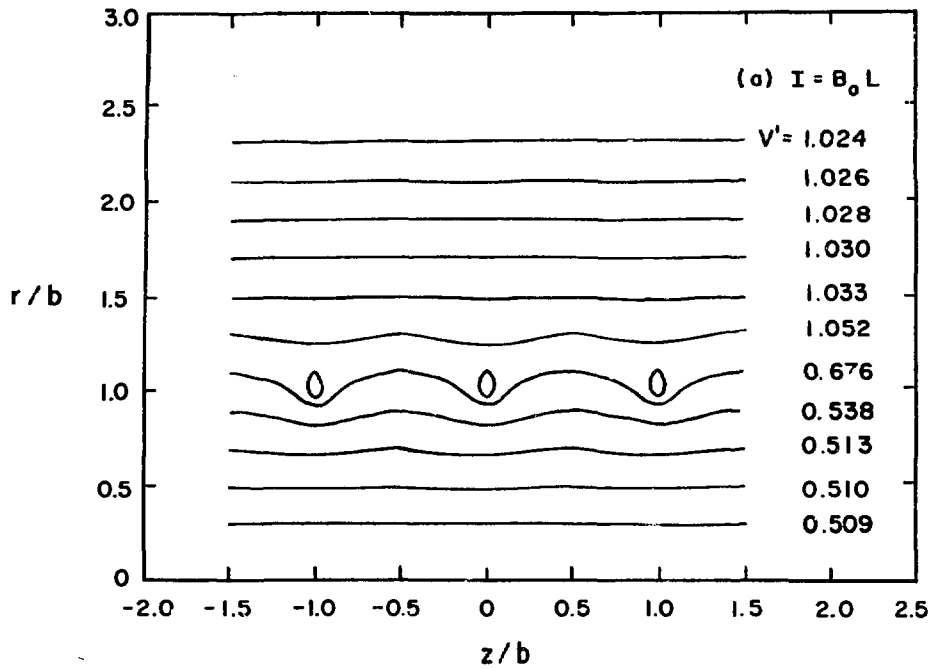


Fig. 3.
Field-line plots for (a) $I = B_0 L$ and
(b) $I = 3 B_0 L$.

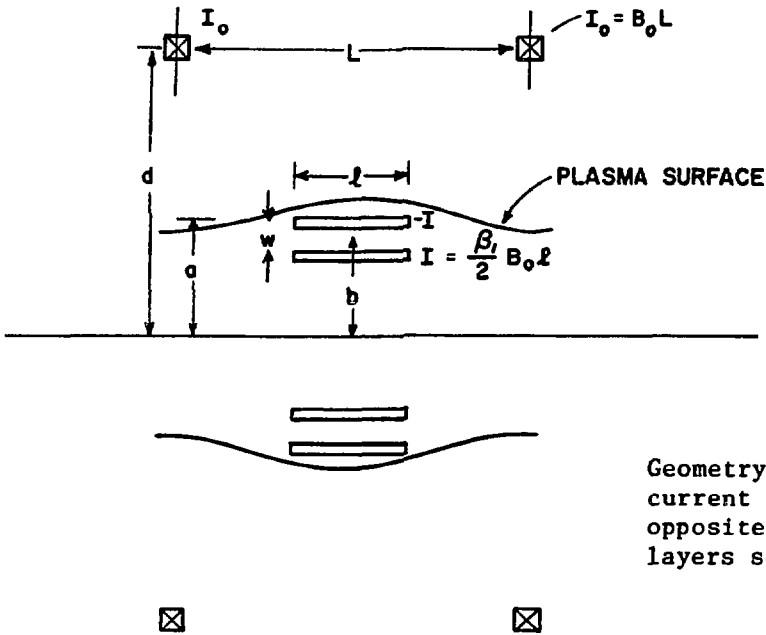


Fig. 4. Geometry of ELMO. The hot-electron current is denoted by I and flows in opposite directions on concentric layers separated by w .

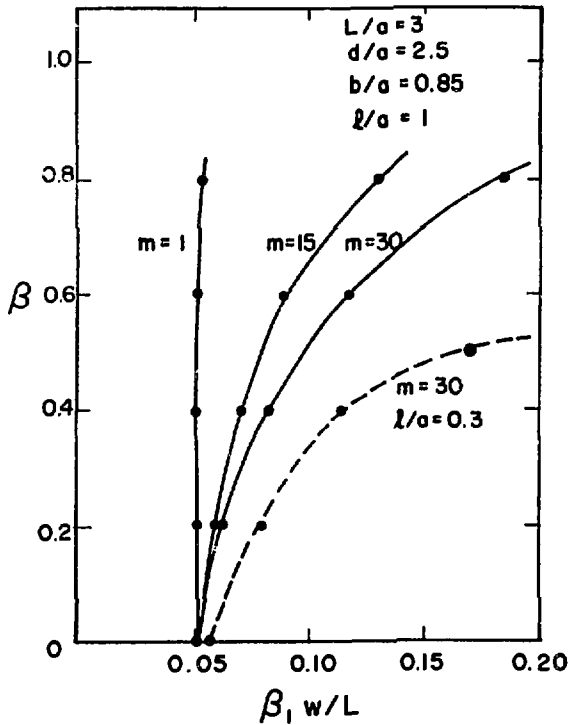


Fig. 5. Stability of ELMO in the sharp-boundary model as a function of β and β_1 ($\beta_1 = \beta$ of the hot-electron annulus), for different m values.

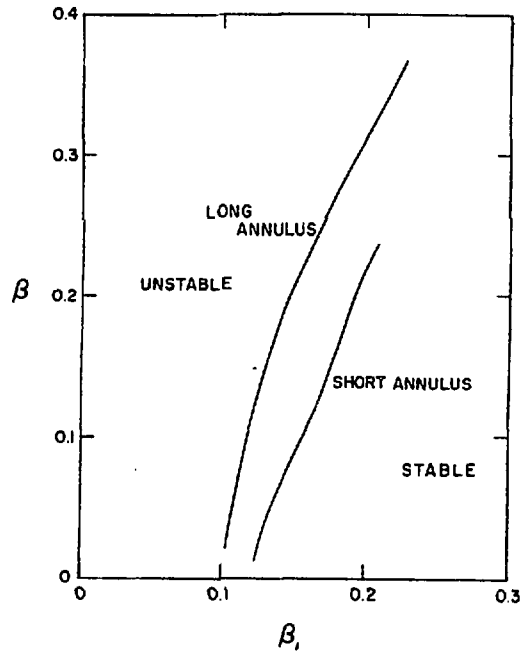


Fig. 6. Stability of the main plasma in ELMO as a function of β and β_1 , from diffuse-profile theory.